FINAL REPORT

Geothermal analysis on Garibaldi Volcanic Belt samples

Geothermal Open Laboratory
(Laboratoire ouvert de géothermie, LOG)

Félix-Antoine Comeau
Mafalda Miranda
Violaine Gascuel
Jasmin Raymond

Institut national de la recherche scientifique (INRS), Centre Eau Terre Environnement

Prepared for the account of:
Steve Grasby

Natural Resources Canada, Geological Survey of Canada

Rapport de recherche R2010

February 16, 2021

Institut national
de la recherche
scientifique

ISBN : 978-2-925559-12-2 (version numérique)

Dépôt légal - Bibliothèque et Archives nationales du Québec, 2025
Dépôt légal - Bibliothèque et Archives Canada, 2025

1- MATERIAL

In total, 21 core plugs were received early January 2020, and the list is provided below (**Table 1**), several of which were received partially damaged, as shown on these photos:

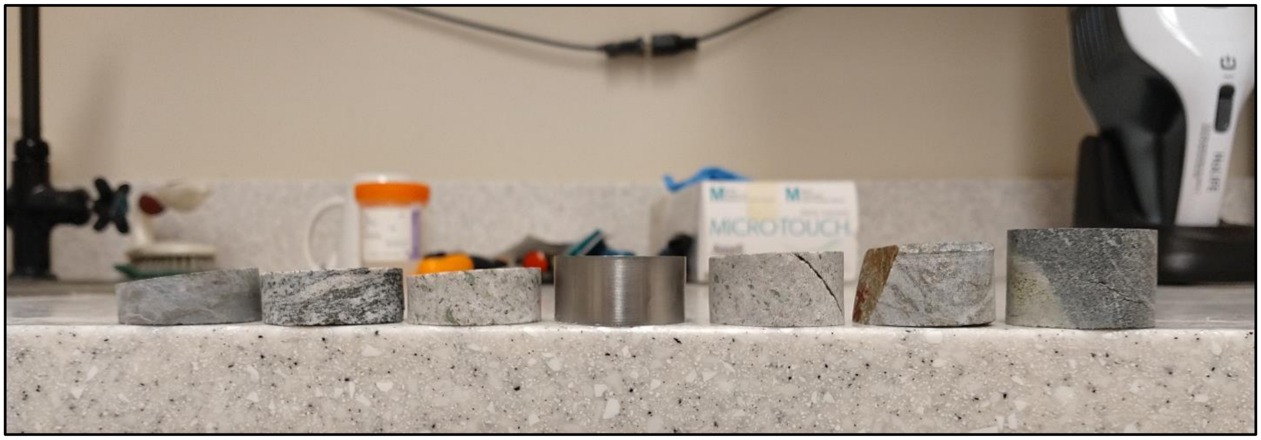

Each sample was measured with an electronic calliper and scale to determine their length, diameter, volume, and weight. Then, the grain volume measurement system of Coretest's AP-608 Permeameter-Porosimeter was used to calculate their density and porosity at room pressure (**Table 1**).

Grain volume measurements are made using helium expansion based on Boyle's Law. Boyle's Law states that the pressure (P) of any ideal gas multiplied by its volume (V) will give a constant value (at a constant temperature). Boyle's Law, as related to core analysis, refers to the ability to determine an unknown volume by expanding a gas of a known pressure and temperature condition into a void space of known volume and using the resulting pressure to calculate the unknown volume. Therefore, by knowing P1, P2, and V2, V1 can be calculated: $V1 = (P2 \cdot V2)/P1$.

Table 1. *List of samples with their respective length and diameter measured with a digital calliper, the calculated bulk volume, and the weight.*

Sample	**Length**	**Diam**	**Volume**	**Weight**	**Density**	**Porosity**
	cm	**cm**	**cm^3**	**g**	**$g\ cm^{-3}$**	**%**
C-634476	1,50	3,81	17,08	45,4	2,66	2,87
C-634477	4,79	3,81	54,67	149,3	2,73	1,19
C-634479	6,09	3,81	69,54	191,9	2,76	1,46
C-634480	3,53	3,82	40,40	115,5	2,86	2,71
C-634481	2,79	3,82	31,88	78,2	2,45	7,35
C-634482	1,91	3,84	22,14	53,1	2,40	5,98
C-634483	2,49	3,81	28,41	55,0	1,94	25,57
C-634484	2,91	3,81	33,10	65,9	1,99	24,98
C-634485	5,03	3,81	57,36	137,2	2,39	11,25
C-634486	6,72	3,81	76,73	146,5	1,91	24,59
C-634487	3,74	3,82	42,87	106,2	2,48	7,93
C-634488	1,93	3,82	22,20	58,6	2,64	4,48
C-634489	2,63	3,81	30,00	80,3	2,68	3,78
C-634490	4,40	3,82	50,33	115,3	2,29	13,88
C-634491	5,42	3,81	61,84	139,5	2,26	13,08
C-634492	3,55	3,81	40,46	103,9	2,57	1,89
C-634493	7,84	3,81	89,54	248,1	2,77	0,70
C-634494	7,78	3,81	88,94	235,6	2,65	2,45
C-634495	7,60	3,81	86,67	55,2	0,64	64,38
C-634498	1,80	3,80	20,41	10,3	0,50	72,65
C-634499	1,77	3,82	20,23	42,8	2,12	14,95

2- METHODS

a. HELIUM POROSITY AND PERMEABILITY MEASUREMENTS

Gas porosity and permeability measurements were made using the Core Test Systems AP-608 Gas combined permeameter and porosimeter. Prior to analyses, samples were first dried at 108°C for at least 48 h, using a Thermolyne oven (Thermo Scientific). AP-608 is a conventional porosimeter applying Boyle's law. The pressure exerted by a mass of helium gas is inversely proportional to the volume of the samples. Measuring the change in helium pressure gives the grain volume porosity value results from two measurements, grain volume and bulk volume. A digital calliper is used to measure the length and diameter and calculate the bulk sample volume (**Table 1**). Initial helium pressure is set at 200 psi.

Permeability is measured with the same instrument based on the transient pressure decay method and results are expressed in m^2 or Darcy units. Permeability values (K kling; **Table 2**) are obtained with Darcy's law considering Klinkenberg correction for gas slippage directly done by the instrument. Three distinct confining pressures were applied, 500, 2 500 and 5 000 psig, for permeability assessment and an additional porosity measurement was made at the same time.
Note that sample C-634495 was destroyed during analysis at 2 500 psi. It had an extremely high porosity (60-65%) and was therefore very fragile.

Table 2. *Porosity and permeability obtained at different confining pressures and measured with the gas combined permeameter and porosimeter.*

Sample	P conf (psig)	Porosity (%)	K klink (mD)
C-634476	502,2	2,10	0,001
	2 447,4	1,31	0,000
	5 002,8	1,12	0,000
C-634477	500,9	0,63	0,004
	2 452,5	0,19	0,000
	4 995,8	0,16	0,000
C-634479	513,4	0,24	0,001
	2 448,4	0,06	0,000
	4 992,3	0,03	0,000
C-634480	497,2	1,19	0,002
	2 410,3	0,61	0,000
	4 945,9	0,53	0,000
C-634481	506,7	6,99	0,042
	2 508,0	6,13	0,017
	4 976,2	5,45	0,009
C-634482	512,3	8,11	0,000
	2 499,7	5,82	0,000
	5 003,7	5,39	0,000

C-634483	514,7	24,56	69,19
	2 501,5	22,70	32,28
	5 014,0	21,77	22,66
C-634484	522,6	21,56	1 260,59
	2 520,2	19,35	801,93
	4 989,2	18,65	551,28
C-634485	509,6	10,27	2,20
	2 450,2	9,85	0,88
	4 982,2	9,62	0,52
C-634486	524,4	23,20	2 685,46
	2 458,3	22,41	2 513,51
	5 036,3	22,03	2 209,92
C-634487	503,3	7,46	0,061
	2 509,3	6,45	0,016
	5 004,0	5,81	0,008
C-634488	508,3	4,23	0,020
	2 435,2	2,67	0,051
	5 032,4	1,88	0,001
C-634489	506,4	3,22	0,002
	2 472,3	1,87	0,000
	4 982,9	0,98	0,000
C-634490	513,9	13,56	0,61
	2 501,9	12,65	0,48
	5 059,8	12,20	0,43
C-634491	521,6	7,88	0,005
	2 488,6	4,87	0,002
	5 087,2	2,60	0,001
C-634492	498,8	1,35	0,000
	2 514,1	0,79	0,000
	5 048,8	0,50	0,000
C-634493	511,9	0,52	0,001
	2 454,0	0,33	0,000
	5 064,8	0,21	0,000
C-634494	520,3	0,81	0,000
	2 527,0	0,50	0,000
	5 032,1	0,36	0,000
C-634495	526,1	60,90	1 803,63
C-634499	501,2	14,81	0,000
	2 446,9	14,17	0,000
	5 024,7	13,72	0,000

b. THERMAL CONDUCTIVITY SCANNER

A thermal conductivity scanner with an infrared heat source made by LGM Lippmann is used for transient thermal conductivity and diffusivity analysis of core samples at room temperature. The instrument relies on the optical scanning technique developed by Popov (1999) to conduct the analysis. A moving optical head with an infrared heat source and temperature sensors can scan thermal properties along the sample (Jorand et al., 2013). The temperature sensors are located before and after the heat source to measure unperturbed, or cold, and perturbed, or hot, temperature from which the thermal conductivity and diffusivity are deduced according to comparative measurements performed on reference samples placed before and after the rock sample. Flat and cylindrical sample faces of 40 to 500 mm in length can be analyzed along a scan line that has been painted with black enamel to ensure proper infrared absorption to heat the sample. A dry rock sample is placed between reference materials and measurements can be achieved at a scanning speed of 5 mm s^{-1}. The transient heat transfer analysis achieved with the thermal conductivity scanner has a small depth of penetration and allows a local evaluation of thermal properties along the scan line to identify potential heterogeneity. Finally, a mean value of thermal conductivity and diffusivity distributed along the scanning line of the sample was calculated (**Table 3**).

The measured samples must always be at the same height as the reference samples. This adds an additional challenge to perform measurements on cylindrical samples as their curvature would place the scan line lower than the reference samples if the core was directly placed on the instrument. Metal washer placed under both the cores and reference samples were used to solve this issue. However, due to the thermal proprieties of these washers, the heat signal is perturbed near the edges of the samples. The thermal proprieties measured near the edges of the samples were thus not taken into consideration, reducing the analyzed length. The results from smaller samples measured on their cylindrical surface may thus not be as reliable as the analyzed length can be less than a centimetre. They were marked as such in **Table 3**. When the sample was smaller than an inch, the profile was done on one of its extremities (flat diamond cut). Otherwise, the analysis was performed along the cylindrical surface. In this case, whenever possible, four measures were carried on four different sides of the samples. For sample C-634493, two runs were measured on the same side of the sample and were averaged before averaging with the results obtained on the other sides.

Lastly, to get the best conditions for measurements, the sample surface must be as smooth as possible. Thus, measurements done on samples with visible porosity are of lesser quality and are marked as such in **Table 3**.

Table 3. *Thermal conductivity and diffusivity values obtained with the infrared scanner.*

Sample	**Surface**	**Inhomogeneity factor**	**Thermal conductivity ($W\ m^{-1}K^{-1}$)**		**Thermal Diffusivity ($mm^2\ s^{-1}$)**	
			Mean	**St. Dev.**	**Mean**	**St. Dev.**
C-634476	flat diamond cut	0.032	2.39	-	1.08	-
C-634477	core cylindrical	0.178	3.22	0.30	1.62	0.21
C-634479	core cylindrical	0.082	2.28	0.12	1.07	0.04
C-634480	core cylindrical	0.056	2.65	0.26	1.15	0.11
C-634481 [1]	core cylindrical	0.067	3.52	-	1.26	-
C-634482	flat diamond cut	0.087	1.97	0.04	1.01	0.01
C-634483	flat diamond cut	0.030	0.89	-	0.50	-
C-634484 [1,2]	core cylindrical	0.018	1.07	-	0.79	-
C-634485	core cylindrical	0.094	1.31	0.10	0.98	0.45
C-634486 [2]	core cylindrical	0.143	1.01	0.13	0.77	0.16
C-634487 [1]	core cylindrical	0.048	1.34	0.07	0.72	0.08
C-634488	flat diamond cut	0.213	2.62	0.16	0.85	0.09
C-634489	flat diamond cut	0.164	2.64	-	1.14	-
C-634490	core cylindrical	0.109	1.61	0.70	0.87	0.08
C-634491 [2]	core cylindrical	0.009	1.37	-	0.87	-
C-634492	core cylindrical	0.049	2.98	-	1.53	-
C-634493	core cylindrical	0.176	2.36	0.10	1.18	0.07
C-634494	core cylindrical	0.088	1.98	0.11	1.03	0.06
C-634498 [1]	core cylindrical	0.145	0.65	0.00	0.48	0.04
C-634499 [2]	flat diamond cut	0.229	0.90	-	0.45	-

[1] Less reliable measure due to small sample length.

[2] Less reliable measure due to visible porosity (samples must be smooth for optimum use of the TCS)

c. GUARDED HEAT FLOW METER

A FOX-50 guarded heat flow meter from Laser Comp is installed to perform thermal conductivity analysis of core plug samples in steady state at controlled temperature. The instrument consists of parallel round conducting plates with a guard insulation cylinder. Plates are equipped with thermoelectric Peltier elements and water flow cooled heat sink to control temperature. The sample is placed between the plates maintained at given temperature to establish a steady-state heat transfer rate across the sample. Heat flow transducers evaluate the heat flux based on the electric signal of the elements to deduce the temperature gradient and calculate the thermal conductivity with an accuracy of 3 % (Filla and Slifka, 1997).

Cylindrical shaped samples with a diameter of 25 to 61 mm and a maximum thickness of 25 mm can be analyzed with the guarded heat flow meter to determine thermal conductivity under a range of 0.1 to 10 $Wm^{-1}K^{-1}$ at controlled temperature from -10 to 190°C. The guarded heat flow meter allows establishing a vertical steady-state heat flow across the whole sample in order to determine its bulk thermal conductivity (**Table 4**). A temperature difference of 10 ºC is imposed on both plates and successive data acquisition cycles grouped in blocks are run until the temperature of the upper and lower plates and transducer signals satisfy all the necessary equilibrium criteria to declare the sample in thermal equilibrium. Thermal conductivity is evaluated posteriorly. The equilibrium criteria are as follows:

- Temperature equilibrium (TE) criterion: the average temperature of each plate must be equal to the set point temperature within the chosen TE value. The default is 1 ºC;
- Semi-equilibrium (SE) criterion is met when transducers average signals are equal within the SE chosen value. The default is 200 μV;
- Percent equilibrium (PE) criterion: the average signal of the transducers must be equal to the value of the PE criterion chosen. The default value is 2 %;
- Number of blocks of PE refers to the number of blocks satisfying the PE criterion required to declare that thermal equilibrium has been reached and results can be calculated;
- Inflection criterion is met when the transducers average signal of successive data acquisition cycles is equal to zero. Only when this final criterion is met, the equilibrium is declared, and the results are calculated.

Each plate must meet each of these equilibrium criteria independently. Moreover, as the equipment is composed by two conducting plates, two different thermal conductivity values are obtained. The final thermal conductivity is the average between the values obtained in the upper and lower plate. Due to the roughness of the samples' surfaces, a thin rubber pad was placed between the sample and the plates. Additionally, a film of silicone paste of about 0.1 mm was smeared on both samples' surfaces to improve the thermal contact and decrease the thermal resistance. The thermal conductivity value obtained from the device was posteriorly corrected for the effect of the pads.

The volumetric heat capacity, with an accuracy of 5 %, of the sample can additionally be deduced from the temperature measurements during the transient heat transfer period before the sample temperature reach equilibrium. The volumetric heat capacity is made in a twofold procedure independent of thermal conductivity evaluation. No temperature difference is imposed on the conductive plates, but two analyses at different temperatures are required. When the semi-equilibrium criterion is reached for the first temperature imposed, the equipment jumps to the following temperature set point. Volumetric heat capacity is evaluated based on the time that the sample takes to reach a new semi-equilibrium criterion.

Initial analyses were also performed on all samples to evaluate the thermal conductivity at temperatures of 20, 60, 100, 140 and 180 ºC (**Table 4**), and volumetric heat capacity at 20, 60, 100, 140 and 160 ºC (**Table 4**). It is important to indicate that volumetric heat capacity cannot be analyzed at 180 ºC due to limitations of the equipment, and therefore the 160 ºC temperature was evaluated instead.

Table 4. *Thermal conductivity (TC, W m^{-1} K^{-1}) and heat capacity (HC, MJ m^{-3} K^{-1}) on dry samples as a function of temperature, and evaluated with the FOX-50 guarded heat flow meter.*

	Temperature (°C)										
	20		**60**		**100**		**140**		**160**	**180**	
Sample	**TC**	**HC**	**TC**	**HC**	**TC**	**HC**	**TC**	**HC**	**HC**	**TC**	**Comments**
C-634479	1,229	2,182	1,258	2,448	1,343	2,529	1,385	2,776	2,845	1,427	Surfaces are not parallel, no porosity visible
C-634481	1,021	1,672	1,067	1,918	1,121	2,06	1,171	2,335	2,362	1,202	Surfaces are not parallel, no porosity visible
C-634483	0,690	1,502	0,706	1,719	0,711	1,727	0,709	1,936	2,135	0,644	Parallel surfaces, highly porous
C-634485	1,118	1,818	1,156	2,065	1,173	2,151	1,211	2,46	2,583	1,229	Parallel surfaces, some visible porosity
C-634486	0,840	1,439	0,866	1,676	0,876	1,739	0,892	2,027	2,094	0,887	Parallel surfaces, highly porous
C-634487	1,013	1,811	1,145	2,005	1,222	2,156	1,248	2,327	2,413	1,311	Surfaces are not parallel, no porosity visible
C-634489	3,000	2,112	2,853	2,403	2,903	2,552	2,765	2,817	2,889	2,593	Good quality, parallel surfaces, no porosity visible
C-634490	1,377	1,683	1,410	1,889	1,423	2,052	1,438	2,383	2,418	1,411	Good quality, parallel surfaces, no porosity visible
C-634491	1,254	1,878	1,296	2,111	2,237	2,237	1,322	2,439	2,498	1,347	Surfaces are not parallel, some visible porosity
C-634492	3,254	1,982	2,993	2,275	2,762	2,388	2,675	2,742	2,865	2,557	Good quality, parallel surfaces, no porosity visible
C-634493	2,877	2,037	2,699	2,353	2,631	2,462	2,580	2,745	2,944	2,450	Good quality, parallel surfaces, no porosity visible
C-634494	1,313	1,957	1,373	2,23	1,416	2,359	1,462	2,698	2,773	1,525	Surfaces are not parallel, no porosity visible
C-634495	0,176	5,886	0,176	7,029	0,169	7,307	0,178	8,604	9,242	0,160	Surfaces are not parallel, highly porous
C-634498	0,139	4,016	0,145	4,833	0,153	5,079	0,166	5,923	6,215	0,166	Surfaces are not parallel, highly porous
C-634499	0,746	1,585	0,766	1,799	0,785	1,879	0,818	2,138	2,265	0,848	Surfaces are not parallel, some visible porosity

Subsequent analyses under saturated water conditions were then carried out on 11 samples showing the highest porosity values. For this purpose, the samples were placed in a vacuum chamber at negative pressure using a pump and filled with distilled water for 3 days in order to saturate the pores of the rock samples with water. A Parafilm™ was used to wrap the cylindrical surface of the samples in order to prevent major water losses during the analyses. Thermal conductivity and volumetric heat capacity were evaluated on the saturated samples at room temperature (20 °C), and the results obtained are given in **Table 5**.

Table 5. *Thermal conductivity (TC) and volumetric heat capacity (HC) of saturated samples at room temperature (20 °C) evaluated with the FOX-50 guarded heat flow meter.*

Sample	**TC** (W m^{-1} K^{-1})	**HC** (MJ m^{-3} K^{-1})	**Comments**
C-634481	1,39	1,96	Surfaces are not parallel, no porosity visible
C-634483	1,35	1,72	Parallel surfaces, highly porous
C-634485	1,74	2,02	Parallel surfaces, some visible porosity
C-634486	1,38	2,19	Parallel surfaces, highly porous
C-634487	1,07	2,02	Surfaces are not parallel, no porosity visible
C-634489	2,94	2,29	Good quality, parallel surfaces, no porosity visible
C-634490	1,97	2,15	Good quality, parallel surfaces, no porosity visible
C-634491	1,71	2,09	Surfaces are not parallel, some visible porosity
C-634495	0,48	1,39	Surfaces are not parallel, highly porous
C-634498	0,47	1,15	Surfaces are not parallel, highly porous
C-634499	1,28	2,21	Surfaces are not parallel, some visible porosity

3- COMPARISON OF ANALYSIS RESULTS

The **Table 6** compare the thermal conductivity (TC) analysis results between the thermal conductivity scanner (TCS) and the guarded heat flow meter (FOX). Most of the relative differences are within a 25 % window between the results of the two instruments, as already observed by Giordano et al. (2019) and Miranda et al. (2020). The highest differences between both instruments are highlighted in grey in **Table 6**, and reached ~75 %.

Those differences can be explained by a poor sample preparation, and inherent heterogeneity associated with the rock itself. Although belonging to the same rock type, each equipment used a specific sample dataset. Therefore, taking into consideration the results presented in this report and the ones obtained by Giordano et al. (2019) and Miranda et al. (2020), both steady-state and transient methods should be used together to avoid a biased evaluation of the thermal conductivity.

The quality of samples shall, therefore, be considered when evaluating the reliability of measurements, depending on sample size and porosity when using the TCS and the parallelism and smoothness of the faces when using the FOX.

Table 6. *Difference of the thermal conductivity (TC) analysis results between the thermal conductivity scanner (TCS) and the guarded heat flow meter (FOX-50) on dry samples.*

Sample	TC (W m^{-1} K^{-1})		
	FOX	TCS	TCS vs FOX (%)
C-634479	1,229	2,280	46,096
C-634481	1,021	3,520	70,994
C-634483	0,690	0,890	22,472
C-634485	1,118	1,310	14,656
C-634486	0,840	1,010	16,832
C-634487	1,013	1,340	24,403
C-634489	3,000	2,640	-13,636
C-634490	1,377	1,610	14,472
C-634491	1,254	1,370	8,467
C-634492	3,254	2,980	-9,195
C-634493	2,877	2,360	-21,907
C-634494	1,313	1,980	33,687
C-634495	0,176	--	
C-634498	0,139	0,650	78,615
C-634499	0,746	0,900	17,111

In order to highlight the role played by porosity on the thermal conductivity and volumetric heat capacity, analyses made for the 11 most porous samples were compared under dry and water-saturated condition. **Table 7** shows thermal conductivity differences of more than 50% for the majority of the samples. Variations in volumetric heat capacity are modest and generally below 20%. It should be noted that a low thermal conductivity and a high heat capacity were obtained for samples C-634495 and C-634498 under water-saturated condition (highlighted in grey in **Table 7**), which is explained by their high porosity (> 60%). Thus, their porous nature made the analyses difficult and the results should therefore be taken with caution.

Table 7. *Difference of thermal conductivity (TC) and heat capacity (HP) between dry and saturated samples at room temperature (20 °C) evaluated with the guarded heat flow meter (FOX-50).*

Sample	**TC** (W m^{-1} K^{-1}) **dry**	**sat**	**Diff.** (%)	**HC** (MJ m^{-3} K^{-1}) **dry**	**sat**	**Diff.** (%)	**Comments**
C-634481	1,02	1,39	-36	1,67	1,96	-17	Surfaces are not parallel, no porosity visible
C-634483	0,69	1,35	-96	1,50	1,72	-15	Parallel surfaces, highly porous
C-634485	1,12	1,74	-56	1,82	2,02	-11	Parallel surfaces, some visible porosity
C-634486	0,84	1,38	-64	1,44	2,19	-52	Parallel surfaces, highly porous
C-634487	1,01	1,07	-6	1,81	2,02	-12	Surfaces are not parallel, no porosity visible
C-634489	3,00	2,94	2	2,11	2,29	-8	Good quality, parallel surfaces, no porosity visible
C-634490	1,38	1,97	-43	1,68	2,15	-28	Good quality, parallel surfaces, no porosity visible
C-634491	1,25	1,71	-36	1,88	2,09	-11	Surfaces are not parallel, some visible porosity
C-634495	0,18	0,48	-173	5,89	1,39	76	Surfaces are not parallel, highly porous
C-634498	0,14	0,47	-238	4,02	1,15	71	Surfaces are not parallel, highly porous
C-634499	0,75	1,28	-72	1,59	2,21	-39	Surfaces are not parallel, some visible porosity

4- REFERENCES

Filla, B.J. and Slifka, A.J., 1997. Thermal conductivity measurements of pyroceram 9606 using a high-temperature guarded-hot-plate. Proceedings of the 24th International Thermal Conductivity Conference. Lancaster: 85–96.

Giordano, N., Chicco, J., Mandrone, G., Verdoya, M. and Wheeler, W.H., 2019. Comparing transient and steady-state methods for the thermal conductivity characterization of a borehole heat exchanger field in Bergen, Norway. Environmental Earth Sciences 78: 460. https://doi.org/10.1007/s12665-019-8397-7

Jorand, R., Vogt, C., Marquart, G. and Clauser, C., 2013. Effective thermal conductivity of heterogeneous rocks from laboratory experiments and numerical modeling. JGR: Solid Earth 118(10) : 5225–5235. https://doi.org/10.1002/jgrb.50373

Miranda, M.M., Giordano, N., Raymond, J, Pereira, A.J.S.C., Dezayes, C., 2020. Thermophysical properties of surficial rocks: a tool to characterize geothermal resources of remote northern regions. Geothermal Energy 8:4. https://doi.org/10.1186/s40517-020-0159-y

Popov, Y.A., Pribnow, D.F.C., Sass, J.H., Williams, C.F., Burkhardt, H., 1999. Characterization of rock thermal conductivity by high-resolution optical scanning. Geothermics 28(2): 253-276. https://doi.org/10.1016/S0375-6505(99)00007-3